Faraday Discussions

Controllable membrane remodeling by a modified fragment of the apoptotic protein Bax

Journal:	*Faraday Discussions*
Manuscript ID	FD-ART-05-2020-000070.R1
Article Type:	Paper
Date Submitted by the Author:	19-Aug-2020

Complete List of Authors:	Schaefer, Katherine ; University of Missouri Columbia College of Arts and Science, Physics and Astronomy Grau, Brayan; University of Tennessee, Biochemistry & Cellular and Molecular Biology; Universitat de Valencia, Departament de Bioquímica i Biologia Molecular, Estructura de Recerca Interdisciplinar en Biotecnologia i Biomedicina (ERI BioTecMed), Moore, Nicolas; University of Tennessee, Biochemistry & Cellular and Molecular Biology Mingarro, Ismael; Universitat de Valencia, Departament de Bioquímica i Biologia Molecular, Estructura de Recerca Interdisciplinar en Biotecnologia i Biomedicina (ERI BioTecMed), King, Gavin; University of Missouri Columbia College of Arts and Science, Physics and Astronomy; University of Missouri, Department of Biochemistry Barrera, Francisco; University of Tennessee, Biochemistry & Cellular and Molecular Biology

Controllable membrane remodeling by a modified fragment of the apoptotic protein Bax

Katherine G. Schaefer[1,*], Brayan Grau[2,3,*], Nicolas Moore[2], Ismael Mingarro[3], Gavin M. King[1,4] and Francisco N. Barrera[2]

[1] Department of Physics and Astronomy, University of Missouri, Columbia, MO 65211, USA

[2] Department of Biochemistry & Cellular and Molecular Biology, University of Tennessee, Knoxville, 37996, USA.

[3] Departament de Bioquímica i Biologia Molecular, Estructura de Recerca Interdisciplinar en Biotecnologia i Biomedicina (ERI BioTecMed), Universitat de València. E-46100 Burjassot, Spain.

[4] Department of Biochemistry, University of Missouri, Columbia, Missouri, 65211, USA.

* These authors contributed equally

Correspondence: fbarrera@utk.edu, kinggm@missouri.edu

Abstract

Intrinsic apoptosis is orchestrated by a group of proteins that mediate the coordinated disruption of mitochondrial membranes. Bax is a multi-domain protein that, upon activation, disrupts the integrity of the mitochondrial outer membrane by forming pores. We strategically introduced glutamic acids into a short sequence of the Bax protein that constitutively creates membrane pores. The resulting BaxE5 peptide efficiently permeabilizes membranes at acidic pH, showing low permeabilization at neutral pH. Atomic force microscopy (AFM) imaging showed that at acidic pH BaxE5 established several membrane remodeling modalities that progressively disturbed the integrity of the lipid bilayer. The AFM data offers vistas on the membrane disruption process, which starts with pore formation and progresses through localized exposure of membrane monolayers leading to stable and small (height ~16 Å) lipid-peptide complexes. The different types of membrane morphology observed in the presence of BaxE5 suggest that the peptide can establish different types of membrane interactions. BaxE5 adopts a rare unstructured conformation when bound to membranes, which might facilitate the dynamic transition between those different states, and then promote membrane digestion.

Introduction

Apoptosis is a programmed cell death mechanism that plays an important role in multicellular organisms. The intrinsic or mitochondrial apoptosis process is triggered by the Bcl2 (B cell lymohoma-2)-family, which governs mitochondrial outer membrane permeabilization. Within this family, pro- and anti-apoptotic members mediate cell survival through a complex network of interactions about which insufficient knowledge is available. Bax (Bcl2 associated protein X) is a pro-apoptotic multi-domain protein that is activated by tBid (truncated BH3 interacting-domain death agonist) to permeabilize the mitochondrial outer membrane. Specifically, Bax forms a membrane pore that releases pro-apoptotic factors from the mitochondrial intermembrane space.[1] It has been previously found out that Bax$^{\alpha 5}$, a peptide comprising helix 5 plus a fraction of helix 6 of Bax, both of which are involved in dimerization and pore formation, can directly disrupt membranes, bypassing the need for activation for membrane pore formation.[2,3]

Controlled membrane pore formation has the potential to become a therapeutic tool, as leakage of contents out of the diseased cell could cause their demise. However, this possibility has been precluded by a lack of specificity, as pore formation cannot be efficiently prevented in healthy cells. Here, efforts are described towards controllable pore formation triggered by acidic pH. pH-dependency is a promising property for therapeutic applications, as diseased states characterized by extracellular acidosis include aggressive solid tumors,[4] arthritic inflammation,[5] and sepsis.[6]

The Barrera laboratory has previously used judicious introduction of acidic residues (aspartic or glutamic acid) to i) design peptides that use the acidity of tumors to target the membranes of cancer cells,[7,8] and ii) design membrane peptides that bind and activate the receptor tyrosine kinase EphA2.[9] Here, we modified Bax$^{\alpha 5}$ to create a peptide that disrupts membranes selectively at acidic pH. To this end, glutamic acid residues were strategically introduced into the Bax$^{\alpha 5}$ peptide sequence. The modified peptide exhibits pH-dependent membrane disruption, which results in major bilayer remodeling.

Materials and Methods

Peptide preparation. The BaxE5 peptide was chemically synthesized using F-moc chemistry. Peptide purity was assessed by HPLC and MALDI-TOF. Peptide stocks were prepared by dissolving the powder using MilliQ water, where the pH was raised to pH 8 with an aliquot of NaOH. Peptide stock concentration was calculated by absorbance of the single Tyr residue in the sequence (**Figure 1**), using a molar extinction coefficient of 1490 M^{-1} cm^{-1}.

Circular Dichroism (CD). CD samples were prepared by diluting concentrated stocks of peptide in 1 mM phosphate buffer at pH 7.5. Large unilamellar vesicles (LUVs) of the lipid POPC (1-palmitoyl-2-oleoyl-glycero-3-phosphocholine, from Avanti Polar Lipids) were formed by extrusion, using 100 nm pore filters. BaxE5 was incubated with LUVs to reach a peptide:lipid molar ratio of 1:200 in 1 mM sodium phosphate buffer (NaP_i) pH 7.5 for at least 45 min. After peptide-lipid incubation, pH was modified by adding sodium acetate buffer (pH 4.3), for 5 mM final buffer concentration and 5 μM final peptide concentration, followed by another 45 min incubation. CD measurements were performed on a Jasco J-815 spectropolarimeter at 25 ºC in a 2 mm cuvette. The appropriate lipid-derived backgrounds were subtracted from data recorded. Values were normalized to molar ellipticity (millidegrees).

Leakage assay. Dried POPC lipids were rehydrated with 20 mM Sulforhodamine B (SRB, Thermo) and extruded using 200 nm filters. Excess of free SRB was removed by using Sephadex G-25 desalting columns (GE Healthcare). The elution of SRB encapsulated in POPC vesicles was done using 1 mM NaP_i buffer pH 7.5. Peptide dilutions for each assay were made from fresh 10 mM stock in 1 mM NaP_i pH 7.5. Final vesicle concentration was 90 μM in 200 μL final volume. Measurements were performed using a BioTek Cytation V Imaging Reader at an excitation wavelength of 485 nm and an emission wavelength of 590 nm. Percentage of leakage was calculated using the following equation:

$$\text{(Equation 1)} \quad \%\ \text{leakage} = \frac{\text{sample} - \text{control}}{\text{triton} - \text{control}} \times 100,$$

where Triton X-100 (10% v/v) was used to induce total leakage, and buffer in the absence of peptide was used as non-leakage control.

Atomic Force Microscopy. 1,2-dioleoyl-sn-glycero-3-phosphocholine (DOPC) (Avanti polar lipids) liposomes were prepared from a chloroform stock. Chloroform was first evaporated using Argon gas to form lipid films which were then placed in a rough vacuum chamber (~0.1 Pa) overnight. An oil-free pump (XDS5, Edwards) was used to prevent backstreaming of oil, a potential contaminant. Samples were sealed with parafilm and stored at -20˚C. When required, a dry lipid stock was swelled in phosphate buffered saline solution (3 mM KCl, 8 mM Na_3PO_4, 140 mM NaCl, pH 7.5) for 60 minutes. After swelling, the lipid solution was extruded 30 times to form unilamellar liposomes (200 nm pore diameter, Liposofast, Avestin). This solution was aliquoted in 5 μL volumes and stored at -80˚C. Final DOPC concentration was approximately 5.5 mM. A volume (5 μL) of BaxE5 stock (31 μM or 33 μM) was added to DOPC at pH 7.5, such that the peptide:lipid molar ratio was either 1:100 or 1:170 and incubated for 5 minutes. The solution was subsequently diluted 1:11 in pH 4.0 buffer (10 mM Hepes, 100 mM KAc) or pH 7.5 buffer (10 mM Hepes, 100 mM Na_3PO_4) and incubated for an additional 10 minutes. At the time of delivery onto the supporting surface the final concentrations of lipid and peptide were, respectively, 1.4 μM and 250 μM for the 1:100 peptide to lipid (P:L) ratio, or 1.5 μM and 250 μM for the 1:170 P:L samples. One hundred μL of solution was deposited onto a freshly cleaved mica surface. This was incubated for 20-30 minutes to allow liposomes to rupture and form a planar bilayer on the surface.[10-12] The sample was then heavily rinsed by exchanging 100 μL of pH 4.0 buffer or pH 7.5 buffer 5-6 times and imaged. For samples originally prepared in pH 7.5 buffer, a series of images were taken. Then the tip was raised from the surface and the buffer exchanged for pH 4.0 imaging buffer (100 μL) 5-6 times and imaged. For control experiments performed with DOPC lipid in the absence of peptide, pH 4.0 buffer was added to DOPC to attain 250 μM, a similar concentration as the peptide samples. This solution was then deposited onto a freshly cleaved mica surface and incubated for 20-30 minutes at room temperature. These samples were rinsed 5-6 times with pH 4.0 buffer, then imaged. All images were obtained in fluid using a commercial instrument (Asylum Research Cypher) and tips (BL-AC40TS, Olympus). The images were acquired in tapping mode, with an estimated tip-sample force less than 100 pN. Analysis of pore-like feature topography was performed using custom software developed in Igor 7 (Wavemetrics, Portland, OR).[13] Smoothed histograms were produced in Igor 7 using Epanechnikov kernel density estimation.

Results

The sequence of the Bax$^{\alpha5}$ peptide contains a single acidic residue. Three additional glutamic acid residues were introduced at non-conserved positions (**Figure 1A**). The resulting BaxE5 peptide is readily soluble in aqueous solution at close to neutral pH. The parental Bax$^{\alpha5}$ peptide permeabilizes lipid bilayers in a concentration-dependent manner. We studied the effect of BaxE5 on membrane integrity measuring its effect on the leakage of sulforhodamine B out of large unilamellar vesicles (LUVs) of the lipid POPC. **Figure 1B** shows that at pH 4, BaxE5 can efficiently release sulforhodamine B at low concentrations. Interestingly, the degree of dye leakage was controlled by pH. At neutral pH inefficient leakage was observed. In contrast, BaxE5 efficiently disrupted membrane integrity at acidic pH, in agreement with the design principle we pursued. We used circular dichroism (CD) to determine the conformation of BaxE5 in the presence of POPC at acidic pH. **Figure 2A** shows that the CD spectra had a minimum at 204 nm, a value typically observed for peptides and proteins in a largely unstructured conformation.[14,15] A shoulder was observed at 222 nm, which indicates that the peptide has a weak α-helical character, in contrast to the original peptide that in aqueous solvent displayed values close to 40% total helical structure, considering both regular and distorted α-helix. [1]We observed that at pH 4.2 the presence of BaxE5 reduced the absorbance at 250 nm of the sample, but no effect was observed at neutral pH (**Figure 2B**). The changes in absorbance possibly result from a reduction of the light the LUVs scatter, and suggest that BaxE5 induces a disruption in the vesicle structure.

Atomic force microscopy (AFM) studies can shed direct light on the nature of peptide-induced membrane disruption.[16-18] Our initial AFM studies focused on samples prepared and deposited on the mica surface in acidic buffer (10 mM Hepes, 100 mM KAc, pH 4.0), corresponding to conditions of high vesicle leakage. **Figure 3** highlights the basic observations. In the presence of the BaxE5 peptide at pH 4, highly localized punctate depressions appeared in the DOPC membrane. Following our previous AFM work characterizing other pore forming peptides,[10-12] these features are likely to be pores or pore precursors, and we will refer to them generally as pore-like features. A control experiment was performed at the same pH without peptide (**Figure 3B**). In this sample the bilayer surface showed no localized depressions. To quantitatively assess membrane disruption, measures of the root-mean-square (RMS) roughness were taken inside 75 nm x 75 nm areas. The RMS roughness was 0.7 Å for the bare membrane and 1.6 Å for the

peptide-disrupted membrane. Line scans further show the dramatic change from a smooth bilayer surface in the absence of peptide (**Figure 3D**) to numerous pore-like depressions in the presence of peptide (**Figure 3C**). The presence of a DOPC lipid bilayer itself was verified by the expected ~50 Å step height from the supporting surface in both samples (**Figure 3E**).[19-21]

We used the custom Hessian blob-detection software to analyze the AFM data and quantify the physical parameters defining the individual pore-like features. The depth histogram (**Figure 3F)** has a single sharp peak at a depth of ~6 Å, with a slight shoulder extending out to 10 Å. However, convolution of the tip with the pore limits the depth measurement, as previously discussed[10,11]. A histogram of area (**Figure 3G**) peaks around 4000 Å^2. If an approximately circular pore geometry is assumed, this gives an effective pore radius of about 36 Å. Single pore-like features demonstrated substantial conformational dynamics over time. **Figure 4** shows an example. Hessian blob analysis was used to measure the radius and depth of the pore-like feature. We observed that the dimensions of the feature fluctuated substantially from image to image. The average radius in the image sequence was 50 ± 6 Å (mean ± standard deviation) and the average depth was 7 ± 2 Å. We note that the precision of the vertical (depth) dimension in AFM is typically ~1 Å.[22] Hence, these observations are not likely to be dominated by noise, but rather genuine topographic changes of the local membrane/lipid structure. Further, duplicate images of the same area (*not shown*), but with the tip scanning in the opposite direction, reproduced similar dimensional changes. For all 10 images in the sequence (trace and retrace), the average radius was 48 ± 8 Å and the average depth was 7 ± 2 Å.

To evaluate pH-dependent lipid remodeling, samples were deposited and incubated at higher pH, using a buffer comprising 10 mM Hepes, 100 mM Na_3PO_4, pH 7.5. **Figure 5A** shows a representative AFM image of the membrane at pH 7.5, where the lipid remained undisturbed. The RMS roughness measurement was 0.8 Å, a similar value (within the estimated error of 0.3 Å) to bilayers in the absence of peptide at pH 4, which exhibited an RMS roughness of 0.7 Å (**Figure 3B)**. Forty-five minutes later, the pH was lowered by washing multiple times with acidic buffer. **Figure 5B** shows the same sample after lowering the pH to 4. The lipid experienced a large-scale disruption, indicating that BaxE5 remained bound to the membrane. Pore-like structures were less common in favor of more widespread disruption. The roughness measurement was 2.8 Å, larger than the roughness shown in **Figure 3A**. The change from distinct pores to

widespread disruption appeared progressive. The nature of membrane disruption exhibited several modalities, from single pore-like features to disruption of the membrane and finally, removal of the bilayer from the mica surface. **Figure 6A** shows an area where the membrane was remodeled and eventually started to detach over the course of imaging. Initial images show pore-like features, which increase in number and size over time. Lace-like structures thinner than the bilayer eventually form until the bilayer has completely disappeared, presumably resuspended into the imaging buffer solution. An interesting phenomenon was that this large-scale destruction was non-uniform on a small scale. **Figure 6B** shows another instance of large membrane disruption. Over time the lipid bilayer in the lower left corner of the image is nearly completely lost, whereas a patch ~100 nm away in the upper right of the images only shows initial signs of disruption (small, punctate features appearing in the membrane in panel C). This may suggest that after rinsing, there is a non-uniform BaxE5 density at the surface. Because both patches were subject to the same imaging conditions, this data acts as an internal control, suggesting that the observed bilayer remodeling is not tip-induced.

The lace-like structures that remained after lipid bilayer digestion continued to undergo degradation. Upon further imaging, these structures began to divide into smaller fragments. **Figure 7** shows the wide-scale spread of these fragments on the surface. A series of images (**Figure 7B**) indicates that these fragments originate from the earlier lace structures. While some fragments seem to detach from the surface (green arrow), others stay bound to the surface (yellow arrow) for the remainder of the experiment. Hessian blob analysis showed that these fragments were homogenous, and had similar height (~16 Å) by the single peak in a height histogram (**Figure 7C**). This height is much smaller than the expected bilayer height of ~50 Å.[21] The volume histogram of these fragments is also sharp, with a peak at 1.3×10^5 Å^3.

Discussion

Peptides that insert into membranes triggered by a pH change have attracted significant attention from the standpoint of basic scientific knowledge as well as for potential therapeutic applications.[23-26] We applied biochemical and biophysical techniques in conjunction with imaging by single molecule AFM to provide quantitative characterization of lipid bilayer remodeling induced by a novel Bax-based peptide that was rationally designed to target membranes at low pH. The BaxE5 peptide disturbs the integrity of lipid membranes, as assessed by leakage experiments. The effect is strongly

dependent of pH, and efficient leakage is only observed at pH 4. Severe membrane disruption is observed at nanomolar concentrations of BaxE5, as show in **Figure 1B**, where the highest concentration used was 500 nM. BaxE5 also induced a change in the absorbance reading (**Figure 2B**), likely resulting from changes in vesicle scattering. While small absorbance changes were observed in the absence of peptide at different pH, these might be merely caused by the different buffers used. Regarding the absorbance decrease observed at acidic pH, since scatter is proportional to vesicle size, the absorbance reduction suggests that BaxE5 disrupts the integrity of lipid vesicles**.**

AFM provides a direct vista into diverse nanoscale structures induced in supported lipid bilayers by peptides and detergents.[18] Examples range from the pores co-localized with membrane-thinned regions induced by a melittin derivative,[11] striations or ribbons formed by the WALP peptides,[27] to large scale cylindrical structures produced by a peptide from the simian immunodeficiency virus.[28] Detergent micelles and other structures, including highly ordered detergent domains within lipid bilayers have also been observed.[29-31] AFM has also been applied to study Bax, and large irregular pores (or membrane voids), with a ~50 nm radius have been observed.[1,32] These pores are significantly larger than those formed by $Bax^{\alpha 5}$.[3] We carried out AFM imaging to investigate how the BaxE5 peptide remodels a lipid bilayer. While no membrane disturbances were observed at neutral pH (**Figure 5A**), under acidic conditions, significant distortion of the otherwise flat supported DOPC lipid bilayers was observed. The bilayer exhibited several discernable stages of remodeling: pore-like features, connected pore-like features (trenches), a large network of lace-like ribbons, and finally, highly localized fragments or membrane bits (see **Figure 8**). This process resulted in most of the lipid bilayer being "digested", and as a consequence being lost into solution. The digestion of the membrane that BaxE5 carries out appears to have important differences to the mechanism detergents use to solubilize lipid bilayers. AFM imaging of detergent solubilization generally shows an all-or-none mechanism, where the bilayer desorbs from the mica surface without clear intermediates.[31,33] This observation contrasts with the several different intermediary membrane morphologies observed for BaxE5.

Pore-like features were observed under acidic conditions but were absent at neutral pH. This pH-dependent AFM observation is reminiscent of another recently studied peptide-lipid system.[10] A relatively narrow distribution of pore-like features were observed, with an average radius of ~ 36 Å, though individual pores exhibited $r > 50$ Å.

We note that the AFM tip geometry is convoluted in these measurements. As a result, the measured pore depths, which varied between approximately 4 and 10 Å, do not reflect true depth due to the finite aspect ratio of the tip (80 Å nominal tip radius). Steric clash between the tip sidewall and the pore perimeter will lead to artificially shallow pore depths.[10,11] Our pore depth measurements therefore represent a lower limit of the real pore depth. The pore-like features often remained static in the minute time-scale (**Figure 4**), suggesting they were coupled to the lower bilayer leaflet, which suppresses lateral diffusion *via* friction from the underlying supporting surface.[34] Based on this observation, we hypothesize that the pore-like features represent membrane indentations that reach at least the center of the bilayer. However, these features could indeed span the entire thickness of the bilayer, and be *bona fide* pores, as the AFM depth measurements correspond to a lower limit.

The depth and area distributions of the pore-like features show a shoulder at higher values (**Figure 3F & G**), which might reveal the transition into larger membrane disruptions. Indeed, in addition to individual pore-like features, larger scale structures were also apparent in the AFM image data. Trenches or joined pore-like features were prevalent, which we propose result from the fusion of independent pore-like features, which might originate at the initial points of attachment of BaxE5 molecules to the bilayer (**Figure 8**). For example, a few trenches can be seen in **Figure 3A** and many such structures are present in **Figure 5B**, some of which span more than 50 nm in lateral extent. Over time, a striking stage of membrane remodeling became apparent, involving large scale lace-like ribbon formations. This result suggests that BaxE5 might assemble into linear oligomers, maybe similar to the line-type aggregates formed by gramicidin A.[35] Lace structures, many of which were over 100 nm in length (**Figure 6**) had a height of ~26 Å above the mica surface. This value is close to half the full bilayer thickness,[36] which implies that the lace structures cannot correspond to bilayer tubes, or a single bilayer. One possibility is that these lace-like structures could be a lipid monolayer passivated by peptides. A less likely possibility is that they could be co-joined cylindrical reverse micelles or similar arrangements.[28]

The final stage of membrane remodeling resulted in small, well dispersed fragments (membrane bits) on the supporting surface. These appeared to be similar to small-scale structures that have been observed in other membrane systems.[18,28] However, in those cases the partially solubilized particles appeared by re-deposition of mixed

micelles, that lead to bilayer formation. Since the height of the bits (16 Å) is less than half of the 50 Å bilayer thickness, the membrane bits observed here probably correspond to a lipo-protein complex. Because of their highly uniform size, these bits likely contain a lipid/peptide mixture of a well-defined stoichiometry. As with the small pores, tip geometry also convolves into volume measurements in AFM. To estimate the magnitude of this effect, a simulated image was created as previously described.[37,38] The AFM tip was modeled as a truncated cone shape with a hemispherical tip (cone angle = 15˚, radius = 80 Å). The test feature was a delta function with the same height as the histogram peak (16 Å). Morphological dilation of the tip with the test feature created a simulated image whose volume was 6.0×10^4 Å^3. Subtracting this value from the experimentally measured volume roughly deconvolves the effect of tip geometry, giving a more realistic peak volume population of 7×10^4 Å^3. We note that this corrected volume is roughly an order of magnitude larger than that of a single BaxE5 monomer, which we estimate to be 4×10^3 Å^3 from the molecular weight and partial specific volume (~0.73 cm^3/g). Based on the measured volume (7×10^4 Å^3), each bit likely contains less than 20 lipid or peptide molecules in total. One possibility is that the bits represent peptide aggregates absent of lipid. We disfavor this option based on the observation of Fig. 7B, as the bits originate from the membrane laces, and therefore likely contain lipid, probably at its core. We speculate that the molecular structure of such bits corresponds to a small stretch of lipid monolayer, lined by peptides (**Figure 8**). However, since the thickness is less than the length of a fully extended DOPC acyl chain, and in fact ~10 Å thinner than the lace structures (compare figures 6D and 7C) we propose that the presence of BaxE5 deforms the lipid acyl chains. This would result in a reduction in the van der Waals interactions that pack the acyl chains in a monolayer. The weakening of this stabilizing interaction will reduce the tendency of lipids to interact laterally. This might be a potential mechanism for the observed membrane digestion by BaxE5. However, further studies are required to validate this model.

The CD data indicates that BaxE5 disrupts membranes in a largely unstructured conformation, with a small helical content. This suggests that the addition of the three E residues (Figure 1) destabilizes helix formation in BaxE5. These mutations are expected to slightly reduce helical content in solution[39]. The majority of peptides that permeabilize membranes are well-structured in the membrane-bound conformation.[23] In most cases these peptides adopt a helical structure, as is the case of the un-modified Bax$^{\alpha5}$ peptide,[2]

while most of the rest adopt beta structure. Indolicidin is one of the rare instances of membrane-disrupting peptides that do not adopt stable secondary structure. Indolicidin, of only 13-aa, is secreted by neutrophils to disrupt the membrane integrity of viruses and bacteria.[40] This peptide is rich in tryptophan residues, and proline (25% of the sequence), in contrast to BaxE5, which contains no tryptophan residues and only one proline. However, a feature shared between indolicidin and BaxE5 is the presence of positively charged residues, as the former has a net charge of +4, while BaxE5 is expected to have a similar +5 charge at acidic pH. However, at neutral pH the unprotonated glutamic acids will yield a close to net neutral peptide. The membrane insertion of other acidic peptides where a drop in pH triggers membrane insertion is thought to be driven by the increase in overall peptide hydrophobicity,[7-9,26,41,42] resulting from the protonation of side chain of acidic residues, and the resulting loss of negative charge. The molecular mechanism of the membrane insertion of BaxE5, on the other hand, might not be purely driven by hydrophobicity, but instead rely on the gain of a net positive charge. Only at acidic pH would BaxE5 be a poly-basic peptide, being similar in nature to other membrane-active peptides such as cell-penetrating peptides.[43,44]

While BaxE5 is a mutant of a single helix of the Bax protein, it might be useful to draw comparisons between the mechanisms the two use to disrupt membranes. Bax is monomeric in solution, and dimerizes in the membrane *en route* to further assemble into oligomers, which are thought to form a toroidal pore.[1] In the pore conformation, the Bax structure contains the latch domain and the core domain, comprising helix 5, which largely corresponds to the BaxE5 sequence. However, pore formation requires Bax to be activated by forming a transient complex with BH3-only proteins. In contrast, for BaxE5 to efficiently disrupt membranes requires "activation" by proton binding to the side chain of glutamic acids, as discussed above. Hence, Bax and BaxE5 use different mechanisms to disrupt membranes. Bax forms large and heterogeneous lipid-lined toroidal pores, after attaching to the membrane in a process that has been suggested to be analogous to a carpet model mechanism.[45,46] BaxE5 might also use a carpet model to initially attach to membranes, which leads to widespread membrane remodeling and a loss of bilayer integrity.

Why does BaxE5 induce such a massive membrane remodeling, resulting in digestion of the bilayer? We suspect that the unstructured conformation of BaxE5 is key for this behavior. Membrane peptides and proteins fold to avoid the steep energetic

penalty of unsatisfied hydrogen bonds and unpaired salt bridges in the membrane.[47-49] Our CD data indicates that BaxE5 bound to the membrane does not form a structure that is significantly stabilized by hydrogen bonds. We hypothesize that BaxE5 remodels the bilayer in search of more energetically stable overall conformation. The linear aggregates of BaxE5 hypothesized in the lace structure would be more stable, but only marginally, and further evolve into the bit structure (**Fig. 7 and 8**). The relative homogeneous properties of the membrane bits suggest a stable conformation.

We show here how the BaxE5 peptide disrupts membranes in a specific acidic pH-triggered fashion. Therefore, BaxE5 has the potential to be developed into a therapeutic tool for cancer, among other diseases. Specifically, aggressive solid tumors are characterized by an acidic extracellular pH.[4,50,51] In fact, a slightly modified version of the Bax$^{\alpha 5}$ peptide causes apoptosis in cell culture, and produces tumor regression in a mammary carcinoma xenograft model.[52] We do not know yet if BaxE5 might kill cells at the mildly acidic pH found in tumors (pH 6.5-7.0). If that occurred, it might digest the membrane of cancer cells, and also microenvironment cells that promote tumor growth and malignancy, including immuno-modulatory cells. If membrane disruption could be made to be specific, peptides causing this effect might be more efficient than peptides that form small membrane pores in acidic conditions, which might be more easily repaired by the cell.[10] While membrane-disrupting peptides have the potential to kill cancer cells, lack of specificity and toxicity have limited their use. In fact, clinical trials of cell-penetrating peptides have often yielded disappointing results.[53] Membrane insertion triggered by acidity might provide the basis for specificity, and prevent damage to healthy tissues. The use of nanocarriers might further reduce off-target effects.[8]

Acknowledgements

This work was partially supported by NIH grant R01GM120642 (to F.N.B), NSF grant 1709792 (to G.M.K.) and Generalitat Valenciana grant PROMETEU/2019/065 (to I.M.). B.G. was recipient of a predoctoral fellowship from the University of Valencia (Atracció de Talent program and Research staff stays program). We thank Kanokporn Chattrakun, Boomer Russell and Justin Westerfield for comments on the manuscript.

Figure 1. BaxE5 selectively disrupts lipid integrity. (A) Sequence of the BaxE5 peptide. Three acidic residues were introduced into the sequence of the $Bax^{\alpha 5}$ peptide, at positions 1, 12 and 30. The acidic glutamic acid residues are shown in red, and basic residues in blue. **(B)** Leakage of sulforhodamine B encapsulated in POPC vesicles were measured at pH 4.0 (red) and pH 7.9 (grey) at different peptide concentrations, expressed as peptide:lipid molar percentage.

Figure 2: BaxE5 disrupts membranes in a largely unstructured conformation. (A) Circular dichroism spectrum of BaxE5 in the presence of POPC vesicles at pH 4.3. The molar lipid to peptide ratio was 200 to 1. **(B)** Effect of BaxE5 in the absorbance at 250 nm in the presence of LUVs at pH 4.5 (red) or 7.2 (grey). Error bars are S.D. $n = 3$ and *, $p = 0.02$.

Figure 3: BaxE5 induces pore-like features. Comparison of a DOPC bilayer imaged at pH 4 in the presence **(A)** and absence **(B)** of peptide. The z-scale is shown by the color bar on the left. Root-mean-square (RMS) roughness was measured inside 75 nm x 75 nm areas (white dashed boxes). Roughness values were 1.6 Å and 0.7 Å for **(A)** and **(B)**, respectively. Line scans **(C)** and **(D)** are profiles through the image data (blue dashed lines in **(A)** and **(B)**, respectively). A pore-like feature is indicated **(A & C**, arrow**)**. **(E)** An additional line scan, indicated by dashed red line in **(A)**, reveals the approximately 50 Å height of the lipid bilayer. Hessian blob analysis was performed over **(A)**, identifying pore-like features. Salient geometrical properties of the N=41 pore-like features were collected into histograms, showing the distribution of apparent pore depth **(F)**, which has a sharp peak around 6 Å, and area **(G)**, which peaks at around 4000 $Å^2$.

Figure 4: Conformational dynamics of a single pore-like feature. Image sequence of DOPC in the presence of BaxE5 at pH 4. The data show a single pore-like feature undergoing structural variations over 7 minutes. Topographical characteristics were determined in each image using the Hessian blob algorithm, which outputs feature depth, area, and perimeter. One such perimeter is shown (t=0 panel, red line). Assuming

circularity, areas can be converted to feature radius. The calculated radius (R) and depth (D) are shown for each image.

Figure 5: Membrane disruption is only observed at acidic pH. A DOPC bilayer was first imaged in the presence of BaxE5 at pH 7.5 **(A)**. After approximately 45 minutes, the pH was lowered to 4.0 by washing with acidic buffer. This pH change caused substantial remodeling of the lipid **(B)**. The RMS roughnesses measured inside a 75 nm x 75 nm area (white dashed boxes) were 0.8 Å and 2.8 Å in **(A)** and **(B)**, respectively. Line scans are shown for pH 7.5 **(C)** and pH 4.0 **(D)**.

Figure 6: Severe membrane remodeling by BaxE5 over time with spatially heterogeneous behavior. (A) A time sequence of images shows a bilayer at t=0 s initially continuous, but with punctate and localized depressions, indicative of pore-like features. At times $t \geq 155$ s lace-like structures emerged. Over time, these features appeared more widespread and the continuous lipid bilayer was lost. Panel **(B)** shows that this behavior was spatially inhomogeneous. While the lipid patch in the lower left is being disrupted in the presence of peptide, the lipid patch located in the upper right corner of the same image, remains essentially undisturbed. **(C)** Three hundred and ten seconds later the lower left patch has been completely disrupted, while the second patch (upper right) is only showing initial signs, in the form of pore-like features. **(D)** A line scan through the image in panel **(C)** shows that the lace-like structures are fairly uniform in height (about 26 Å) and lower than the bilayer. The scale bar of are 100 nm applies to all panels. All experiments were performed at pH 4.

Figure 7: Final stages of bilayer digestion. The leftover lace-like structures further degraded into smaller fragments of roughly uniform size **(A)**. Evidence that these features originate from the lace structures is shown by zoomed in images taken over time, where features are seen to directly divide. Some of the fragments appear to dissociate from the surface **(B**, green arrow**)**; whereas many others remain surface-bound upon division **(B**, yellow arrow**)**. **(C)** Histograms of the heights and volumes of these fragments (N=1051) as determined via Hessian blob analysis. A single peak is

located in each distribution at ~16 Å and ~1.3×10^5 Å^3 for height and volume, respectively.

Figure 8. Cartoon model describing the different stages of membrane remodeling caused by BaxE5. At acidic pH, the peptide initially induces the formation of pore-like, circular membrane depressions. These membrane features appear to converge, creating membrane trenches. At later times, or at higher BaxE5 concentrations, thin lace-like ribbons with the approximate thickness of a monolayer are observed. Finally, membrane ribbons are digested into thin membrane bits. Our data cannot exclude that the pore-like features correspond to *bona fide* pores. BaxE5 is shown in red, lipid in blue, and the mica surface in black.

Bibliography

1 Cosentino, K. & Garcia-Saez, A. J. Bax and Bak Pores: Are We Closing the Circle? *Trends Cell Biol* **27**, 266-275 (2017).

2 Garcia-Saez, A. J. *et al.* Peptides derived from apoptotic Bax and Bid reproduce the poration activity of the parent full-length proteins. *Biophys J* **88**, 3976-3990 (2005).

3 Garcia-Saez, A. J. *et al.* Peptides corresponding to helices 5 and 6 of Bax can independently form large lipid pores. *Febs J* **273**, 971-981 (2006).

4 Estrella, V. *et al.* Acidity generated by the tumor microenvironment drives local invasion. *Cancer Res* **73**, 1524-1535 (2013).

5 Andreev, O. A. *et al.* Mechanism and uses of a membrane peptide that targets tumors and other acidic tissues in vivo. *Proc.Natl Acad.Sci.U.S.A.* **104**, 7893-7898 (2007).

6 Henry, K. E. *et al.* Demarcation of Sepsis-Induced Peripheral and Central Acidosis with pH-Low Insertion Cyclic (pHLIC) Peptide. *J Nucl Med* (2020).

7 Nguyen, V. P., Alves, D. S., Scott, H. L., Davis, F. L. & Barrera, F. N. A Novel Soluble Peptide with pH-Responsive Membrane Insertion. *Biochemistry* **54**, 6567-6575 (2015).

8 Nguyen, V. P. *et al.* Mechanistic insights into the pH-dependent membrane peptide ATRAM. *J Control Release* **298**, 142-153 (2019).

9 Alves, D. S. *et al.* A novel pH-dependent membrane peptide that binds to EphA2 and inhibits cell migration. *Elife* **7**, doi:10.7554/eLife.36645 (2018).

10 Kim, S. Y. *et al.* Mechanism of Action of Peptides That Cause the pH-Triggered Macromolecular Poration of Lipid Bilayers. *Journal of the American Chemical Society* **141**, 6706-6718 (2019).

11 Pittman, A. E., Marsh, B. P. & King, G. M. Conformations and Dynamic Transitions of a Melittin Derivative That Forms Macromolecule-Sized Pores in Lipid Bilayers. *Langmuir* **34**, 8393-8399, doi:10.1021/acs.langmuir.8b00804 (2018).

12 Li, S. J. *et al.* Potent Macromolecule-Sized Poration of Lipid Bilayers by the Macrolittins, A Synthetically Evolved Family of Pore-Forming Peptides. *J Am Chem Soc* **140**, 6441-6447, doi:10.1021/jacs.8b03026 (2018).

13 Marsh, B. P., Chada, N., Sanganna Gari, R. R., Sigdel, K. P. & King, G. M. The Hessian Blob Algorithm: Precise Particle Detection in Atomic Force Microscopy Imagery. *Sci Rep* **8**, 978, doi:10.1038/s41598-018-19379-x (2018).

14 Kelly, S. M., Jess, T. J. & Price, N. C. How to study proteins by circular dichroism. *Biochim.Biophys.Acta.* **1751**, 119-139 (2005).

15 Kelly, S. M. & Price, N. The use of Circular Dichroism in the investigation of protein structure and function. *Current Protein and Peptide Letters* **1**, 349-384 (2000).

16 Rinia, H. A. & de Kruijff, B. Imaging domains in model membranes with atomic force microscopy. *FEBS Lett* **504**, 194-199, doi:10.1016/s0014-5793(01)02704-1 (2001).

17 Meincken, M., Holroyd, D. L. & Rautenbach, M. Atomic force microscopy study of the effect of antimicrobial peptides on the cell envelope of Escherichia coli. *Antimicrob Agents Chemother* **49**, 4085-4092, doi:10.1128/AAC.49.10.4085-4092.2005 (2005).

18 El Kirat, K., Morandat, S. & Dufrene, Y. F. Nanoscale analysis of supported lipid bilayers using atomic force microscopy. *Bba-Biomembranes* **1798**, 750-765, doi:10.1016/j.bbamem.2009.07.026 (2010).

19 Muller, D. J. & Engel, A. The height of biomolecules measured with the atomic force microscope depends on electrostatic interactions. *Biophys J* **73**, 1633-1644 (1997).

20 Sanganna Gari, R. R., Frey, N. C., Mao, C., Randall, L. L. & King, G. M. Dynamic structure of the translocon SecYEG in membrane: direct single molecule observations. *J Biol Chem* **288**, 16848-16854, doi:10.1074/jbc.M113.471870 (2013).

21 Attwood, S. J., Choi, Y. & Leonenko, Z. Preparation of DOPC and DPPC Supported Planar Lipid Bilayers for Atomic Force Microscopy and Atomic Force Spectroscopy. *Int J Mol Sci* **14**, 3514-3539 (2013).

22 Bippes, C. A. & Muller, D. J. High-resolution atomic force microscopy and spectroscopy of native membrane proteins. *Rep Prog Phys* **74**, doi:Artn 086601 10.1088/0034-4885/74/8/086601 (2011).

23 Guha, S., Ghimire, J., Wu, E. & Wimley, W. C. Mechanistic Landscape of Membrane-Permeabilizing Peptides. *Chem Rev* **119**, 6040-6085 (2019).

24 Bechinger, B. Towards membrane protein design: pH-sensitive topology of histidine-containing polypeptides. *J Mol Biol* **263**, 768-775 (1996).

25 Li, W., Nicol, F. & Szoka, F. C., Jr. GALA: a designed synthetic pH-responsive amphipathic peptide with applications in drug and gene delivery. *Adv Drug Deliv Rev* **56**, 967-985 (2004).

26 Deacon, J. C., Engelman, D. M. & Barrera, F. N. Targeting acidity in diseased tissues: Mechanism and applications of the membrane-inserting peptide, pHLIP. *Archives of biochemistry and biophysics* **565C**, 40-48, doi:10.1016/j.abb.2014.11.002 (2014).

27 Rinia, H. A. *et al.* Domain formation in phosphatidylcholine bilayers containing transmembrane peptides: Specific effects of flanking residues. *Biochemistry-Us* **41**, 2814-2824, doi:10.1021/bi011796x (2002).

28 El Kirat, K., Dufrene, Y. F., Lins, L. & Brasseur, R. The SIV tilted peptide induces cylindrical reverse micelles in supported lipid bilayers. *Biochemistry-Us* **45**, 9336-9341, doi:10.1021/bi060317x (2006).

29 Liu, J. F., Min, G. & Ducker, W. A. AFM study of adsorption of cationic surfactants and cationic polyelectrolytes at the silica-water interface. *Langmuir* **17**, 4895-4903, doi:DOI 10.1021/la0017936 (2001).

30 Rinia, H. A., Snel, M. M. E., van der Eerden, J. P. J. M. & de Kruijff, B. Visualizing detergent resistant domains in model membranes with atomic force microscopy. *Febs Letters* **501**, 92-96, doi:Doi 10.1016/S0014-5793(01)02636-9 (2001).

31 El Kirat, K., Pardo-Jacques, A. & Morandat, S. Interaction of non-ionic detergents with biomembranes at the nanoscale observed by atomic force microscopy. *Int J Nanotechnol* **5**, 769-783 (2008).

32 Epand, R. F., Martinou, J.-C., Montessuit, S., Epand, R. M. & Yip, C. M. Direct evidence for membrane pore formation by the apoptotic protein Bax. *Biochem Biophys Res Commun* **298**, 744-749 (2002).

33 El Kirat, K., Morandat, S. & Dufrene, Y. F. Nanoscale analysis of supported lipid bilayers using atomic force microscopy. *Biochim Biophys Acta* **1798**, 750-765 (2010).

34 Przybylo, M. *et al.* Lipid diffusion in giant unilamellar vesicles is more than 2 times faster than in supported phospholipid bilayers under identical conditions. *Langmuir* **22**, 9096-9099, doi:10.1021/la061934p (2006).

35 Mou, J., Czajkowsky, D. M. & Shao, Z. Gramicidin A aggregation in supported gel state phosphatidylcholine bilayers. *Biochemistry* **35**, 3222-3226 (1996).

36 Kucerka, N. *et al.* Lipid bilayer structure determined by the simultaneous analysis of neutron and X-ray scattering data. *Biophys J* **95**, 2356-2367 (2008).

37 Sanganna Gari, R. R. *et al.* Direct visualization of the E. coli Sec translocase engaging precursor proteins in lipid bilayers. *Sci Adv* **5**, eaav9404, doi:10.1126/sciadv.aav9404 (2019).

38 Sigdel, K. P., Wilt, L. A., Marsh, B. P., Roberts, A. G. & King, G. M. The conformation and dynamics of P-glycoprotein in a lipid bilayer investigated by atomic force microscopy. *Biochem Pharmacol* **156**, 302-311, doi:10.1016/j.bcp.2018.08.017 (2018).

39 Pace, C. N. & Scholtz, J. M. A helix propensity scale based on experimental studies of peptides and proteins. *Biophys J* **75**, 422-427 (1998).

40 Chan, D. I., Prenner, E. J. & Vogel, H. J. Tryptophan- and arginine-rich antimicrobial peptides: structures and mechanisms of action. *Biochim Biophys Acta* **1758**, 1184-1202 (2006).

41 Scott, H. L., Westerfield, J. M. & Barrera, F. N. Determination of the Membrane Translocation pK of the pH-Low Insertion Peptide. *Biophys J* **113**, 869-879 (2017).

42 Bano-Polo, M., Martinez-Gil, L., Barrera, F. N. & Mingarro, I. Insertion of Bacteriorhodopsin Helix C Variants into Biological Membranes. *Acs Omega* **5**, 556-560 (2020).

43 Fosgerau, K. & Hoffmann, T. Peptide therapeutics: current status and future directions. *Drug Discov Today* **20**, 122-128 (2015).

44 Johnson, R. M., Harrison, S. D. & Maclean, D. Therapeutic applications of cell-penetrating peptides. *Methods in molecular biology (Clifton, N J)* **683**, 535-551 (2011).

45 Uren, R. T., Iyer, S. & Kluck, R. M. Pore formation by dimeric Bak and Bax: an unusual pore? *Philos Trans R Soc Lond B Biol Sci* **372** (2017).

46 Shai, Y. Mechanism of the binding, insertion and destabilization of phospholipid bilayer membranes by alpha-helical antimicrobial and cell non-selective membrane-lytic peptides. *Biochim Biophys Acta* **1462**, 55-70 (1999).

47 Westerfield, J. *et al.* Ions Modulate Key Interactions between pHLIP andLipid Membranes. *Biophys J* **117**, 920-929 (2019).

48 White, S. H., Wimley, W. C., Ladokhin, A. S. & Hristova, K. Protein folding in membranes: determining energetics of peptide-bilayer interactions. *Methods Enzymol.* **295**, 62-87 (1998).

49 Bano-Polo, M. *et al.* Charge pair interactions in transmembrane helices and turn propensity of the connecting sequence promote helical hairpin insertion. *J Mol Biol* **425**, 830-840 (2013).

50 Xu, M., Ma, X., Wei, T., Lu, Z.-X. & Ren, B. In Situ Imaging of Live-Cell Extracellular pH during Cell Apoptosis with Surface-Enhanced Raman Spectroscopy. *Anal Chem* (2018).

51 Anderson, M., Moshnikova, A., Engelman, D. M., Reshetnyak, Y. K. & Andreev, O. A. Probe for the measurement of cell surface pH in vivo and ex vivo. *Proc Natl Acad Sci U S A* **113**, 8177-8181 (2016).

52 Valero, J. G. *et al.* Bax-derived membrane-active peptides act as potent and direct inducers of apoptosis in cancer cells. *J Cell Sci* **124**, 556-564 (2011).

53 Tripathi, P. P., Arami, H., Banga, I., Gupta, J. & Gandhi, S. Cell penetrating peptides in preclinical and clinical cancer diagnosis and therapy. *Oncotarget* **9**, 37252-37267 (2018).

Figure 1

(A)

```
BAX^α5     KGRVVALFYFASKLVLKALSTKVPELIRTK
           1           12              30
BaxE5      EGRVVALFYFAEKLVLKALSTKVPELIRTE
```

(B)

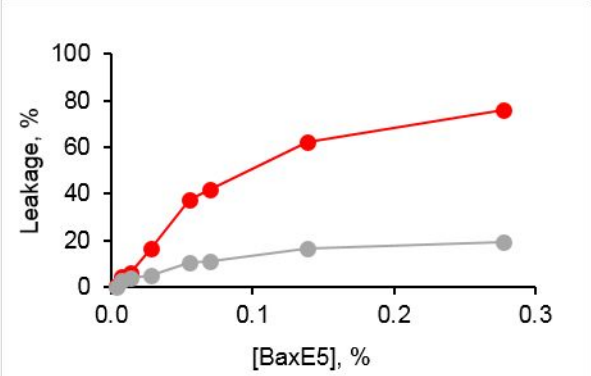

Figure 2

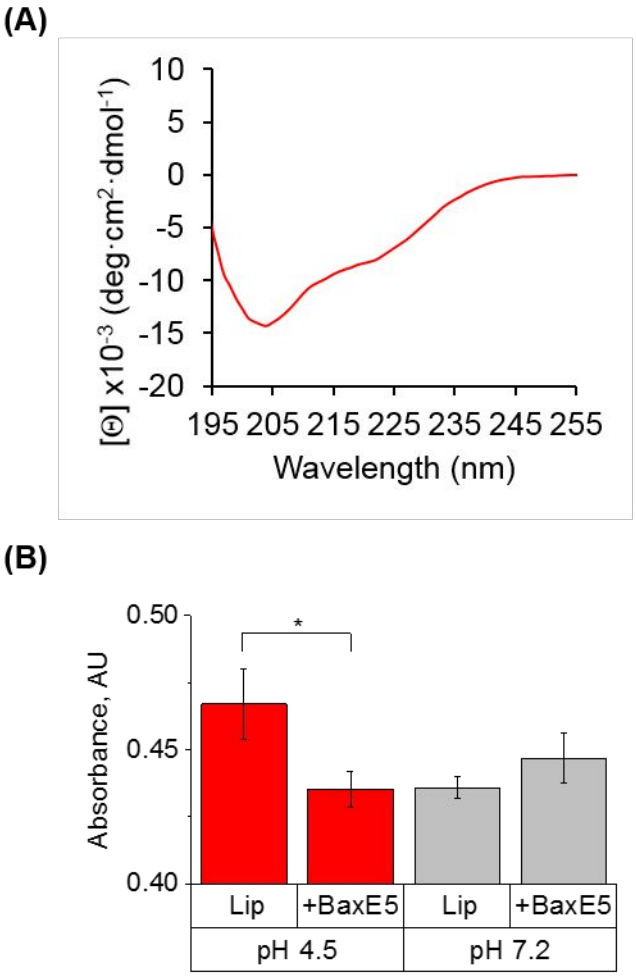
(A)
10
5
0
-5
-10
-15
-20
[Θ] x10-3 (deg·cm2·dmol-1)
195 205 215 225 235 245 255
Wavelength (nm)
(B)
0.50
0.45
0.40
Absorbance, AU
*
Lip
+BaxE5
Lip
+BaxE5
pH 4.5
pH 7.2

Figure 3

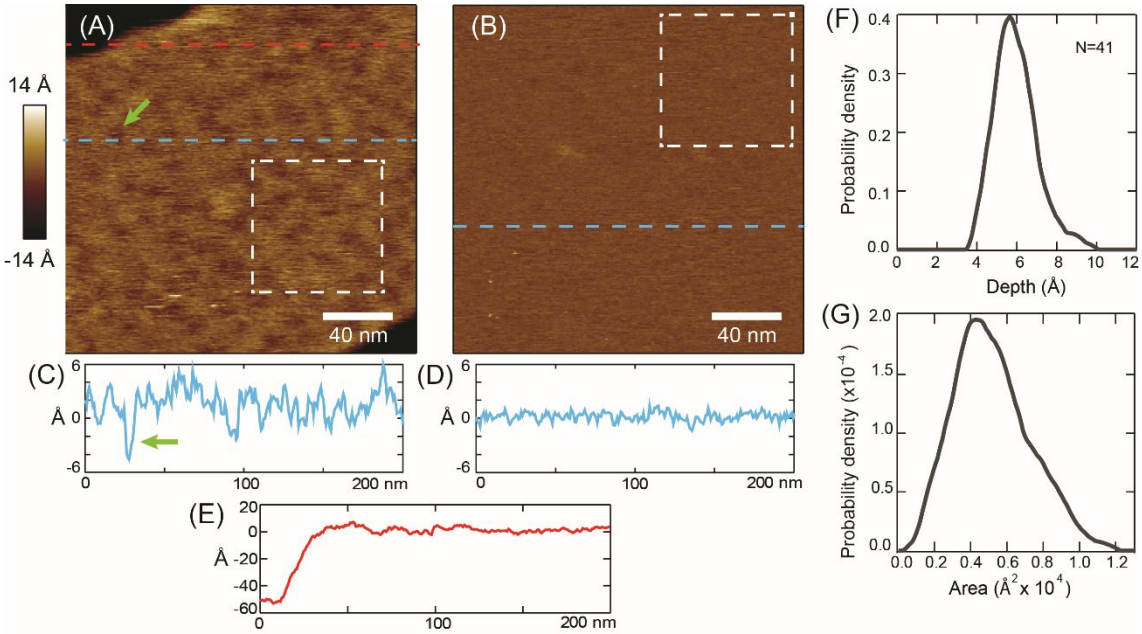
(A)
(B)
14 Å
-14 Å
40 nm
40 nm
(C)
(D)
(E)
Å
200 nm
(F)
N=41
Probability density
Depth (Å)
(G)
Probability density (x10^{-4})
Area (Å^2 x 10^4)

Figure 4

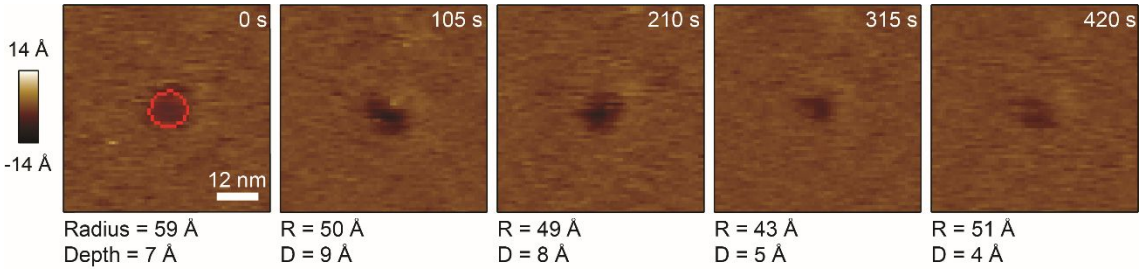
14 Å
-14 Å
0 s
12 nm
105 s
210 s
315 s
420 s
Radius = 59 Å
Depth = 7 Å
R = 50 Å
D = 9 Å
R = 49 Å
D = 8 Å
R = 43 Å
D = 5 Å
R = 51 Å
D = 4 Å

Figure 5

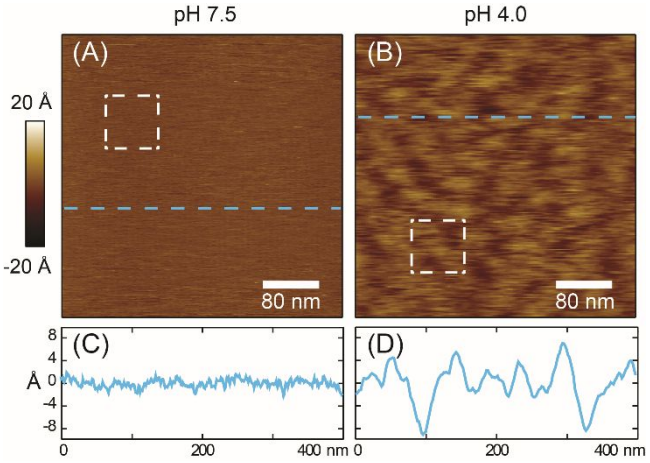
pH 7.5
pH 4.0
(A)
(B)
20 Å
-20 Å
80 nm
80 nm
(C)
(D)
8
4
Å 0
-4
-8
0
200
400 nm
0
200
400 nm

Figure 6

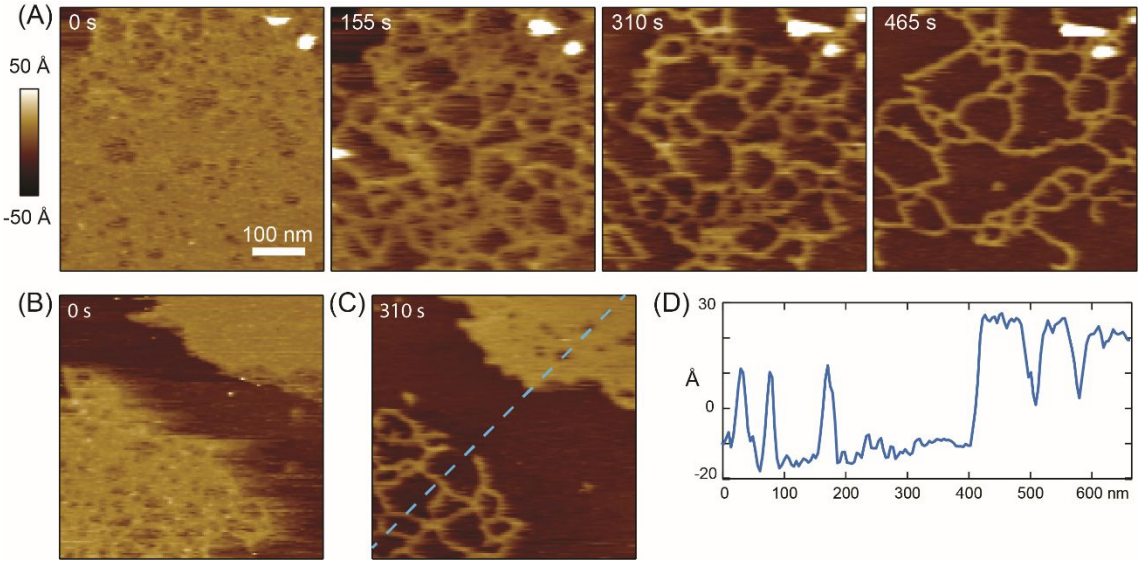
(A)
0 s
155 s
310 s
465 s
50 Å
-50 Å
100 nm
(B)
0 s
(C)
310 s
(D)
30
Å
0
-20
0
100
200
300
400
500
600 nm

Figure 7

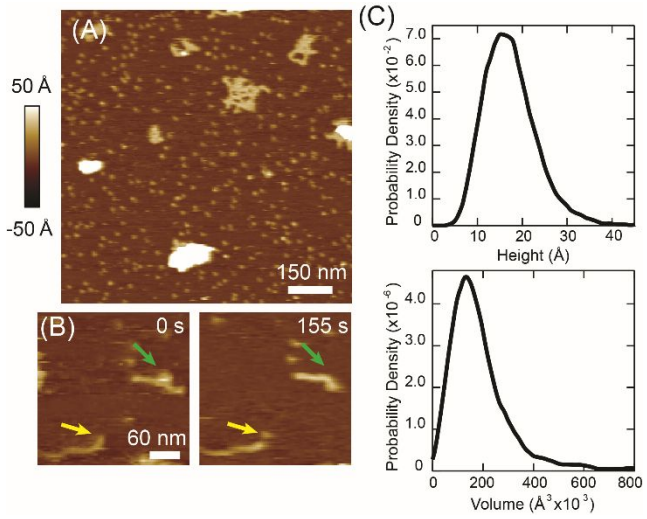
(A)
50 Å
-50 Å
150 nm
(B)
0 s
155 s
60 nm
(C)
Probability Density (x10^{-2})
Height (Å)
Probability Density (x10^{-6})
Volume (Å^{3}x10^3)

Figure 8